ORIGINAL ARTICLE

lajss.org
Latin American Journal of Solids and Structures

www.lajss.org

Reliability-based design of reinforced concrete pipes to satisfy the TEBT

Alex Micael Dantas de Sousa[a]*, Lisiane Pereira Prado[b], Mounir Khalil El Debs[c]

[a]Escola de Engenharia de São Carlos (EESC), Universidade de São Paulo (USP), Av. Trabalhador São Carlense, 400, 13560-590, São Carlos, SP, Brasil. E-mail: alex_dantas@usp.br
[b]Universidade Estadual Paulista (Unesp), Faculdade de Engenharia (FEG), Guaratinguetá, SP, Brasil. E-mail: lisiane.prado@unesp.br
[c]Escola de Engenharia de São Carlos, Universidade de São Paulo, Av. Trabalhador São Carlense, 400, 13560-590, São Carlos, SP, Brasil. E-mail: mkdebs@sc.usp.br

* Corresponding author

https://doi.org/10.1590/1679-78257510

Abstract

Reinforced concrete pipes are usually designed to attend a three-edged-bearing test (TEBT) using the partial safety factors from building structures. This study presents an alternative approach to designing RC pipes based on simplified reliability analyses. The procedure consists of providing curves of failure probability according to the reinforcement areas used in the pipes. The results indicate that RC pipes with simple reinforcement show a failure probability of around 1% with the most traditional design method, even using the partial safety factors from buildings, due to the higher dispersion of the concrete cover and the use of a single reinforcement layer to satisfy different control sections. Meanwhile, RC pipes with double reinforcement show a significantly lower failure probability as each reinforcement layer is designed to satisfy the bending moments from different control sections and due to the larger pipe thickness. In summary, the large randomness of the reinforcement position increases the failure probability of these members compared to traditional building structures.

Keywords

reliability-based design, reinforced concrete pipes, failure probability, three-edge-bearing test.

Graphical Abstract

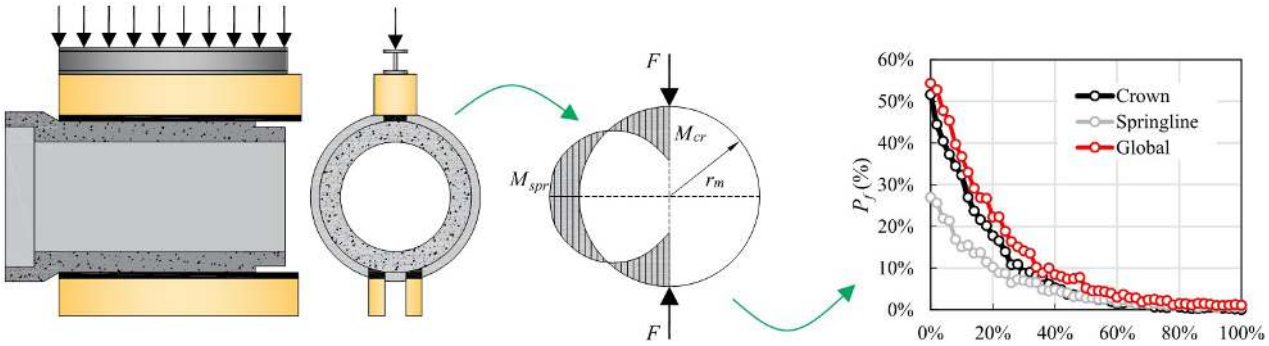

Received February 10, 2023. In revised form June 05, 2023. Accepted June 22, 2023. Available online June 28, 2023.
https://doi.org/10.1590/1679-78257510

Latin American Journal of Solids and Structures. ISSN 1679-7825. Copyright © 2023. This is an Open Access article distributed under the terms of the Creative Commons Attribution License, which permits unrestricted use, distribution, and reproduction in any medium, provided the original work is properly cited.

1 INTRODUCTION

Reinforced concrete pipes are structural members used as rainwater and sanitary sewer conduits in underground infrastructure installations. In countries such as Brazil, these members are of paramount importance for basic sanitation. As in other types of concrete structures, the structural design of pipes is generally developed to meet the ultimate and service limit states (Kataoka et al., 2017; Ramadan et al., 2020).

The AASHTO LRFD Bridge Design Code (AASHTO, 2017) specifies two methods for designing reinforced concrete pipes: Direct Design and Indirect Design. The Direct design method requires the (i) estimation of the earth loads and live loads pressure distributions on the structure for the bedding and installation conditions specified by the engineer; (ii) analyses to determine the internal thrust and internal forces (moments and shear forces) over the pipe and (iii) design the circumferential reinforcement. According to MacDougall et al. (2016), the Indirect Design Method attempts to relate the critical load obtained during three-edge bearing tests (TEBT) conducted by the pipe manufacturer (ASTM C497-13, 2013) to the capacity of the pipes in place through a modification factor named the bedding factor. For instance, the critical load for the American code [5] is specified as the load at which a 0.254 mm crack forms inside the pipe.

Predicting the earth and live load pressure distributions on the structure is somewhat complex. It depends upon the (i) installation process (El Debs, 2003), (ii) soil lateral earth pressure coefficient, (iii) soil cohesion and (iv) the plane of equal settlement (W.-D. Tian, 1989; Y. Tian et al., 2015). Several models were proposed in the literature to estimate the lateral and vertical earth pressures for the design of RC pipes (Das & Seeley, 1975; Ladanyi & Hoyaux, 1969; Marston & Anderson, 1913; Matyas & Davis, 1983; Meyerhof & Adams, 1968; Spangler, 1941; Vesic, 1971). In the Marston−Spangler theory (Marston & Anderson, 1913; Spangler, 1941), vertical earth pressure is assumed to be uniformly distributed. However, some experimental results already indicated that vertical earth pressure is not constant at different points on the pipe (Li, 2009; Shmulevich et al., 1986). Therefore, these characteristics hamper the evaluation of the lateral earth pressures directly on the design of RC pipes.

In summary, it's more frequent designing the pipes to withstand a force corresponding to that resulting from the vertical loads on the tube (in the expected place of installation). Besides, this force shall be divided by the modification factor during the TEBT. The pipe's rating is performed by placing them in resistant classes based on the force to be resisted in the TEBT (El Debs, 2003).

Several studies have been conducted to investigate the behavior of RC pipes with steel fibers as a partial or total substitute for conventional reinforcement (Abolmaali et al., 2012; Figueiredo et al., 2012; Mohamed et al., 2015; Monte et al., 2016; Peyvandi et al., 2014), which usually leads to more efficient structural designs, lower longitudinal reinforcement ratios, improved durability due to increased cover thickness over reinforcement, reduced weight, streamlined geometry (for ease of handling and installation), and enhanced shear resistance (Peyvandi et al., 2013). Others address the behavior of RC pipes with polypropylene fibers as a solution to ensure better response under aggressive environments (Park et al., 2015; Rikabi et al., 2018; Wilson & Abolmaali, 2014). Furthermore, improved design analytical models were developed and experimentally verified for concrete pipes with fibers (Peyvandi et al., 2014). However, no studies address the reliability-based design of reinforced concrete members without fibers, which represents the majority of RC pipes used in practice. Apart from that, the number of studies that discuss the procedure for the design of these elements in a straightforward way is very limited (El Debs, 2003), and the most rational design method should consider the accepted risk by the tube manufacturer, which in this case is related to that of the RC pipe fail on the diametric compression test or TEBT.

This study proposes a more rational approach for designing single-layer and double-layer reinforcements to RC pipes based on simplified reliability analyses. Apart from that, we propose to discuss the influence of the main parameters related to the design of RC pipes: (i) nominal diameter, (ii) pipe wall thickness, (iii) compressive strength of concrete, (iv) yielding strength of reinforcement and (v) the reinforcement concrete covers.

Different design approaches were assessed, and the failure probabilities associated with each one were calculated. The traditional approach (TA) refers to the design of reinforced concrete pipes using partial safety factors from conventional structural elements, such as beams and slabs from buildings. The mean value approach (MVA) determines the longitudinal reinforcement ratio and failure probability, neglecting the partial safety factors and using average values for the material properties. Finally, a rational approach (RA) aims to show an alternative design solution in which the longitudinal reinforcement area to be used depends on the failure probability p_f or failure rate acceptable for reinforced concrete pipes in the TEBT. The Gross Monte Carlo Simulation method was used to estimate the probability of failure of the tubes for each approach. In this work, spreadsheet calculations were used to generate samples and assess the limit state functions (LS) to spread the simplicity of some structural reliability methods. In the end, the FORM method was also applied using the StRAnD software (Beck, 2008) to determine the sensitivity factor of each parameter to the failure probability.

2 BACKGROUND

2.1 Test procedure on the TEBT

The procedure proposed in the Brazilian code ABNT NBR 8890:2018 (2018) is based on the European EN-1916:2002 (EN 1916, 2002) and American guidelines (ASTM C497-13, 2013). This procedure requires the application of a line load uniformly distributed over the upper generatrix of the pipe (crown), while the pipe leans on two closely spaced longitudinal strips over the invert (Figure 1).

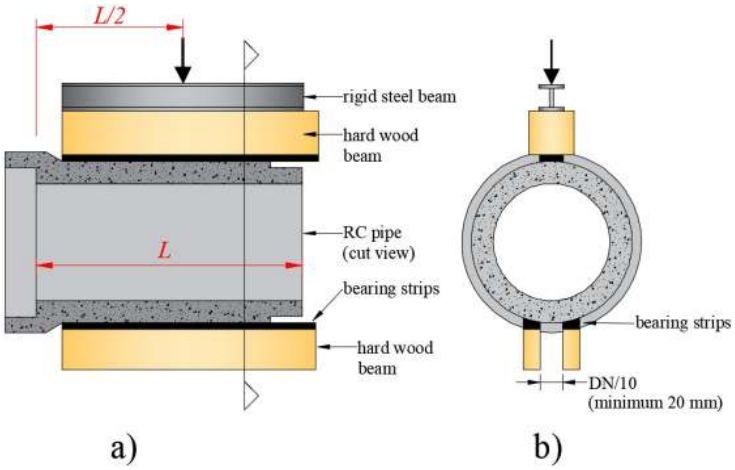

Figure 1 - Test layout for spigot and pocket pipe (SPP): a) cut view in the longitudinal direction and b) cut view in the transversal direction.

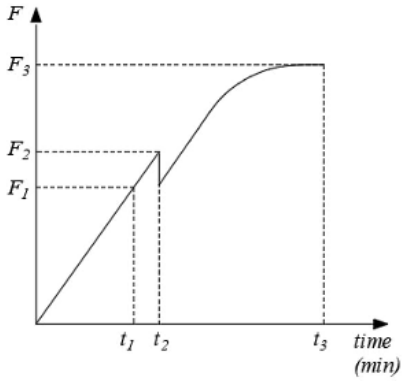

Figure 2 - Typical diametral compression test graph for reinforced concrete pipes. Adapted from ABNT NBR 8890:2018 (ABNT NBR 8890, 2018).

The main loads from the three-edge bearing tests (TEBT) according to the Brazilian code are: (i) the minimum load without visible cracks (F_1); (ii) the cracking load, measured usually by the force drop-down in the load-displacement graph (F_2) and (iii) the maximum force displayed by the measuring device (F_3), which corresponds to the pipe bearing capacity (Figure 2).

2.2 Design approaches for the indirect design method

The design of reinforced concrete pipes shall satisfy service and ultimate limit states. Previous publications dealt with the first (Silva et al., 2008), and this study will focus on the second. The design of RC pipes has some peculiarities. For pipes with only one circular reinforcement layer (simple reinforcement), the longitudinal reinforcement must ensure the required strength in two critical sections: (i) crown and (ii) springline (Figure 3) (El Debs, 2003).

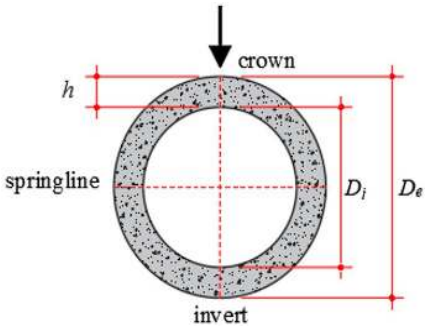

Figure 3 – Definition of the main geometrical parameters and region for RC pipes.

Figure 4 shows the internal force graphs of reinforced concrete pipes for the usual TEBT. The maximum bending moments over the crown and springlines sections are (El Debs, 2003):

$$M_{crown} = \frac{F_r \cdot r_m}{\pi} = 0.318 \cdot F_r \cdot r_m \tag{1}$$

$$M_{springline} = \frac{F_r \cdot r_m}{2} \cdot \left(1 - \frac{2}{\pi}\right) = 0.182 \cdot F \cdot r_m \tag{2}$$

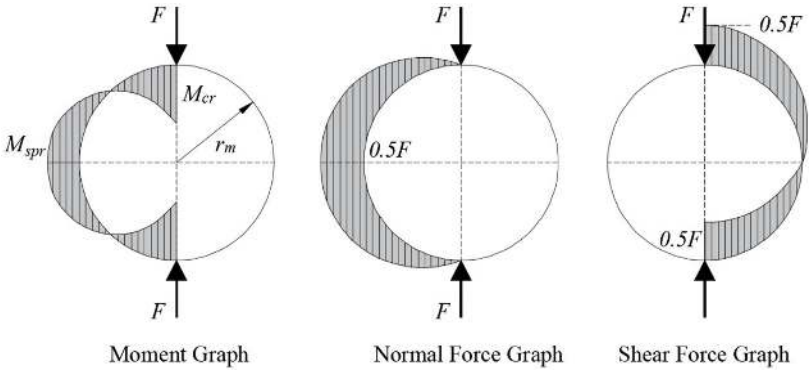

Figure 4 - Internal forces graphs for reinforced concrete pipes under TEBT.

In expressions (1) and (2), M_{crown} is the bending moment at the crown section, $M_{springiline}$ is the bending moment at the springline section, F_r is the distributed load along the pipe length (force per unit length) and r_m is the average radius of the pipe.

Figure 5 shows the main geometrical properties used in the design of RC pipes with simple and double-layer reinforcement. In guidelines for the design of RC pipes (El Debs, 2003), it is usual that pipes with a nominal diameter lower than 1000 mm have only one reinforcement layer. Above this value, it usually provides two-layer reinforcement in design.

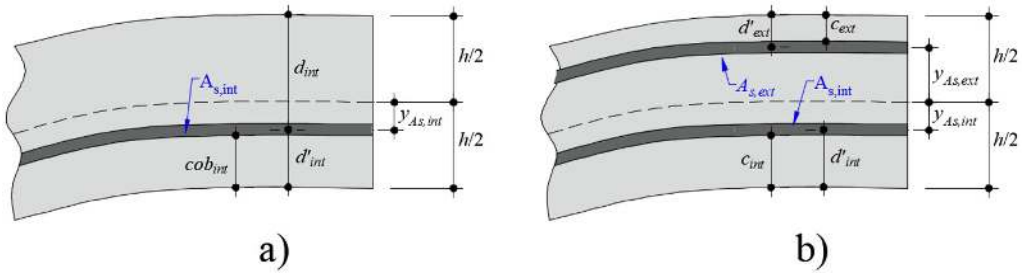

Figure 5 – Reinforcement arrangements for RC pipes with a) simple reinforcement and b) double reinforcement layers. *Adapted from Silva et al. (2018).*

Figure 6 and Figure 7 highlighted the geometric parameters used to calculate the simple reinforcement required in the crown and springline sections. In this study, we compared the reinforcement ratios derived assuming domains 2 and

3, and we verified that differences in reinforcement ratios could be neglected. Therefore, we assumed Domain 3 of strains to provide more straightforward calculations for the neutral axes' depth (*x*).

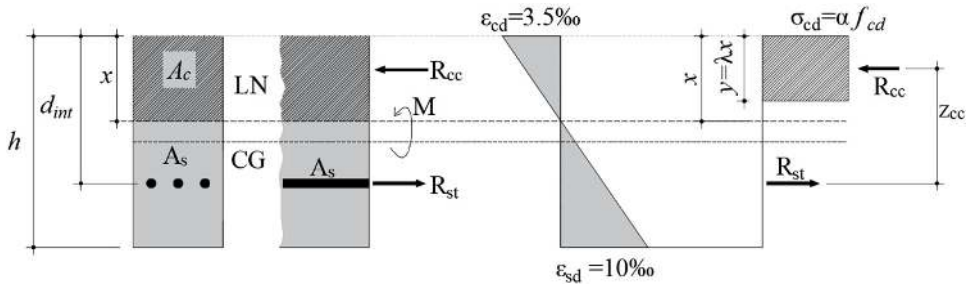

Figure 6 - Detailing of parameters used to design the reinforcement required in the crown section of pipes with one reinforcement layer.

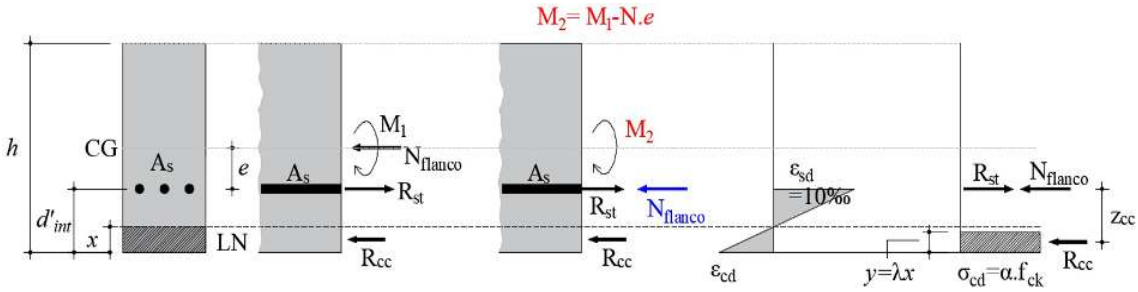

Figure 7 - Detailing of parameters used to design the reinforcement required in the springline section of pipes with only reinforcement layer.

According to ABNT NBR 6118:2014 (ABNT NBR 6118, 2014) (Sections 12.3.3 and 17.2.2), the factors α and λ b shall be calculated as:

$$\begin{aligned} &\lambda = 0.8 \text{ for } f_{ck} \le 50MPa \\ &\lambda = 0.8 - \left(f_{ck} - 50\right)/400, \text{ for } f_{ck} > 50MPa \end{aligned} \tag{3}$$

$$\begin{aligned} &\alpha = 0.85 \text{ for } f_{ck} \le 50MPa \\ &\alpha = 0.85 \cdot \left(1 - \left(f_{ck} - 50\right)/200\right), \text{ for } f_{ck} > 50MPa \end{aligned} \tag{4}$$

Figure 8 and Figure 9 show the geometrical parameters for calculating the inner and external reinforcement layers of RC pipes with double reinforcement. Note that the strains calculated in the crown and springline sections indicate Domain 2 of strains for most cases. In the design of RC pipes with double-layer reinforcement, it is usual that both reinforcements be tensioned in flexure. Consequently, the internal reinforcement $A_{s,int}$ contributes to the resistance at the springline section and the external reinforcement $A_{s,ext}$ does the same for the crown section.

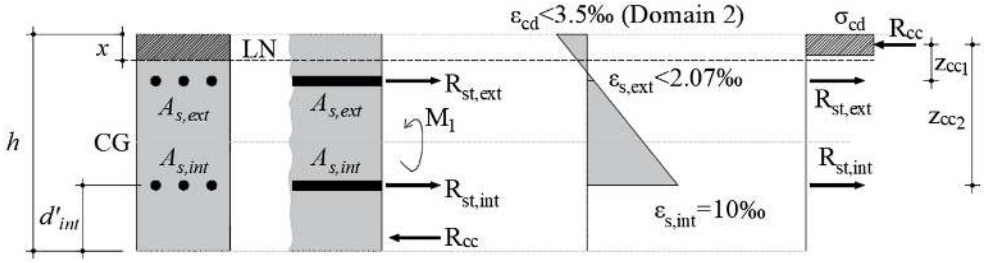

Figure 8 - Detailing of parameters used to design the inner reinforcement required in the crown section of pipes double reinforcement layer.

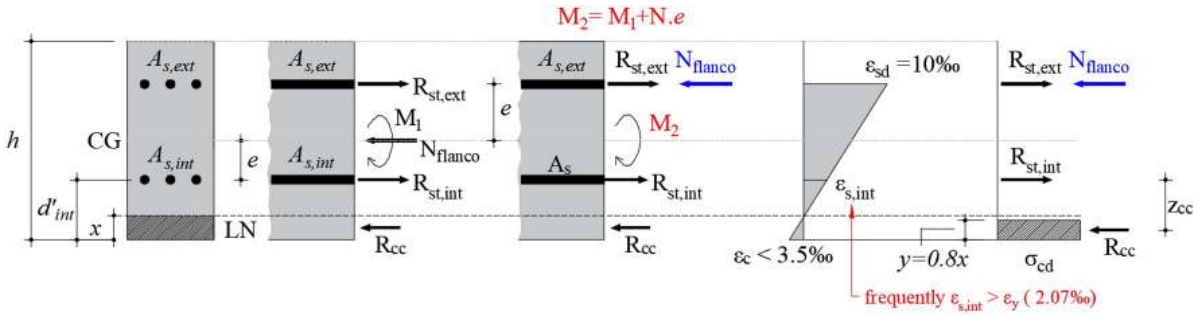

Figure 9 - Detailing of parameters used to design the external reinforcement required in the springline section of pipes double reinforcement layer.

In previous calculations, it was verified that in the design of RC pipes with double reinforcement, external reinforcement's contribution to the crown's flexural strength is very limited (<4%). Therefore, the design of the internal reinforcement of RC pipes with double reinforcement can neglect the external reinforcement contribution in the crown section. For the design of the external reinforcement, we noted that the internal reinforcement shows a significative contribution to the flexural strength in the springline sections, which could lead to reductions of the external reinforcement ratio by more than 50%. However, this would lead to the use of reinforcement rebars very thin, which could hamper reinforcement assembly in the pipes. Since the bending moment over the springline is well lower than over the crown (Figure 4), it is usual to neglect the contribution of the internal reinforcement in the springline section.

Note that, in Figure 9, the bending moment should be increased when the axial force N_{flanco} is offset by e to the position of the external reinforcement. Due to the locations of internal and external reinforcement layers, it is usual that the inner reinforcement layer shows a tensile strain close to or higher than the yielding strain. This observation explains the higher contribution of the internal reinforcement layer in the springline section when considered.

In summary, the area of the inner reinforcement layer $A_{s,int}$ for RC pipes with simple and double reinforcement could be calculated as:

$$A_{s,\text{int}} = \frac{M_{S,crown}}{f_{yd} \cdot z} = \frac{M_{S,crown}}{f_{yd} \cdot \left(d_{l,\text{int}} - \frac{\lambda}{2} \cdot x \right)} \tag{5}$$

$$x = \frac{d_{l,\text{int}} \pm \sqrt{{d_{l,\text{int}}}^2 - 2 \cdot \left(\frac{M_{S,crown}}{b_w \cdot \alpha_c \cdot f_{cd}} \right)}}{\lambda} \tag{6}$$

and the area of reinforcement for the external layer $A_{s,ext}$ can be calculated as (only for RC pipes with double-layer reinforcement):

$$A_{s,ext} = \frac{M_{S,spring,corr}}{f_{yd} \cdot z} = \frac{\left(M_{s,pring} + \frac{N}{2} \cdot e \right)}{f_{yd} \cdot \left(d_{l,ext} - \frac{\lambda}{2} \cdot x \right)} \tag{7}$$

$$x = \frac{d_{l,ext} \pm \sqrt{{d_{l,ext}}^2 - 2 \cdot \left(\frac{M_{S,spring,corr}}{b_w \cdot \alpha_c \cdot f_{cd}} \right)}}{\lambda} \tag{8}$$

At the springline section, the axial force N is equal to $F_r/2$. As the load F_r is a unit of force for a length of 1m, b_w = 1 m or 100 cm in the next sections. e = h/2 - c_{ext} - ϕ_{ext} / 2.

2.3 Aspects needed to be considered in the rational design

Partial safety factors

The design method based on the ABNT NBR 6118:2014 (ABNT NBR 6118, 2014) and ABNT NBR 8681:2003 (ABNT NBR 8681, 2003), here named Traditional Method (TM), uses partial safety factors to ensure adequate safety levels or probability of failure. For actions, the partial safety factor for loadings takes the value γ_f, which derives from the following expression:

$$\gamma_f = \gamma_{f1} \cdot \gamma_{f2} \cdot \gamma_{f3} \tag{9}$$

Where γ_{f1} accounts for the variability of the actions, γ_{f2} accounts for the combination or simultaneity of actions and γ_{f3} considers the model error when evaluating the effects of the actions, the building method or the calculation method used. As the force required in each test F_r is a deterministic quantity according to the tube class (ABNT NBR 8890, 2018), in the design of these elements, the γ_f could be assumed equal to 1 in the Rational Approach (RA).

For materials, the partial safety factors γ_m are related to concrete (γ_c) and reinforcement (γ_s). The coefficient γ_m, whether for concrete or steel, is determined by the following expression:

$$\gamma_m = \gamma_{m1} \cdot \gamma_{m2} \cdot \gamma_{m3} \tag{10}$$

γ_{m1} accounts for the variability of the effective resistance, transforming the characteristic resistance into an extreme value with a lower probability of occurrence; γ_{m2} considers the differences between the effective strength of the structural material and the resistance measured conventionally in standardized specimens; and γ_{m3} considers the current uncertainties in the determination of resistances, either due to defects arising from building methods or due to the calculation method used (model error).

In the design of reinforced concrete structures recommended by ABNT NBR 6118:2014, usually, γ_c and γ_s assume the values of 1.4 and 1.15, respectively. If adequate quality control is established by ABNT NBR 9062: 2017 (ABNT NBR 9062, 2017) (Design of precast concrete structures, Section 8, Materials), γ_c could be reduced to 1.3 and γ_s to 1.1. According to Fusco (Fusco, 2012), the value of γ_c equal to 1.4 derives from the following partial coefficients: γ_{c1} = 1.2; γ_{c2} = 1.08 and γ_{c3} = 1.08. For the concrete, Fusco (2008) explains that γ_{c1} takes into account possible concrete fractions with resistances lower than the specified value $f_{ck,28}$; γ_{c2} considers the different concrete molding, densification and curing processes that exist between the concrete of the structure and the concrete of the standardized specimens; and γ_{c3} takes into account possible localized imperfections in the casting of the structure, as well as possible imperfections in the method of assessing the structural member resistance as a function of the concrete strength.

For reliability analysis, one must use random values for the resistances of concrete and steel and assume γ_f, γ_c and γ_s equal 1. However, for a more rational design of the reinforcements, one can consider the difference between the compressive strength measured in cylindrical specimens and that achieved by the concrete in the tubes after curing. In this case, a correction factor (FC1) equivalent to γ_{c2}, which assumed a value of 1.08, should be considered. Therefore, in the calculation with average values of resistances (MVA = mean values approach), the compressive strength of concrete in the pipe was considered about 8% lower than the average value measured in cylindrical specimens.

Effect of vertical load spreading

The expected moments at crown and invert can be adjusted to account for ring thickness, assuming that the load spreads from the plate loads to the mean depth of the pipe thickness. According to AASHTO LRFD Bridge Design Code (AASHTO, 2017), this effect can be calculated at the bending moment by:

$$M_{thick} = M_{thin} \cdot \left(1 - 0.373 \cdot \frac{t}{R}\right) \tag{11}$$

Where M_{thick} is the adjusted moment, M_{thin} is the moment calculated using the thin ring theory, t is the thickness of the concrete pipe, and R is the radius of the concrete pipe. In this study, this adjustment factor will be named FC2.

To estimate the reduction in the bending moment at this invert/crown section, El Debs (2003) adopts a tube thickness of 1/10 of the average diameter in the calculations and a force propagation to the mean surface of the tube at an angle of 45º. With these considerations, it is possible to calculate the bending moment for a force distributed in a

length of 0.10d_m. Thus, the bending moment in the crowning decreases from 0.318 $F.r_m$ to 0.293$F.r_m$, which means a reduction of approximately 8% in the bending moment of the moment graph. Therefore, FC2 = 1.085 was assumed at the crown section verifications.

Effect of pipe pocket

For RC pipes with ring pockets, there is a beneficial effect of this element for the bearing capacity in the diametrical compression test (or TEBT), since the pocket works such as a stiffer rib coupled to the pipe at one end. Experimental results showed by Silva (2011), indicate that for pipes 800 mm in diameter, with simple reinforcement and 1.5 m in length with pockets, there is an average increase in the bearing capacity per meter of 12.2% compared to pipes without pockets. For pipes of 1200 mm in diameter with pockets, double reinforcement and 1.50 m in length, there is an average increase in the bearing capacity per meter of 4.5%. In this study, we propose to deal with the increase in the bearing capacity by a reduction factor for the maximum bending moments, named here FC3. Since the pocket effect increase for shorter pipes length, we propose the values shown in Table 1 for other dimensions. For intermediate values of pipe length, interpolations from Table 1 can be used.

Table 1 - Reduction factor FC3 due to pocket effect

Pipe length	Simple reinforcement	Double reinforcement
1.5 m	1.122	1.045
1.0 m	1.262	1.175

2.4 Limit state functions

The limit state functions *g* define the failure modes for structural analysis and can be related to ultimate and service limit states. Usually, *g* is defined as:

$$g = R - S \tag{12}$$

Where *R* is the resistance term, and *S* is the load or load effect term for limit state equations. Failure occurs when $g < 0$. For this study, the failure probability consists in seeking the probability that the flexural strength M_R over any pipe section is smaller than the acting bending moment M_S:

$$P_f = P\left[g(X) \le 0\right] = P\left[M_R - M_S \le 0\right] = \int_{D_f} f_X(x) \cdot dx \tag{13}$$

X is a vector that brings together all random variables of resistance and loading, such as geometrical and material parameters used to calculate M_R and M_S. D_f is the failure domain, which represents all combinations of *X* that lead to the failure, defined as:

$$D_f = \left\{ X \middle| g(X) \le 0 \right\} \tag{14}$$

$f_X(x)$ is the joint function or probability density function (pdf) of the random problem variables, which account for the multiple failure modes involved in the structural analyses. From (13) the prediction of the failure probability, P_f requires to evaluate of a multidimensional integral over the failure domain D_f, which can be performed in different ways (Melchers & Beck, 2018): (i) direct integration (less used); (ii) Monte Carlo Simulations (MCS) or (iii) Transformation Methods. A full description of these methods can be found elsewhere (Melchers & Beck, 2018). In traditional designs of RC structures, the failure probability shall satisfy the condition:

$$P_f = \Phi(-\beta) \tag{15}$$

Where Φ is the standard Gaussian function, and β is the required reliability index. In this study, we focus on the ultimate limit states in flexure. Therefore, we used two limit state functions defined as the relation between the difference between the flexural strength M_R and the acting bending moments:

$$g_1(X) = M_{R,crown} - M_{S,crown} \tag{16}$$

$$g_2(X) = M_{R,springline} - M_{S,springline} \tag{17}$$

In the detailed format, the limit state functions (LSF) for the crown section in pipes with simple reinforcement (SR) is:

$$g_1^{SR}(X) = A_{s,\text{int}} \cdot f_y \cdot \left(d_{l,\text{int}} - \frac{\lambda}{2} \cdot x \right) - \frac{0.318}{FC2 \cdot FC3} \cdot F_r \cdot r_m \tag{18}$$

$$g_1^{SR}(X) = A_{s,\text{int}} \cdot f_y \cdot \left(d_{l,\text{int}} - \frac{\lambda}{2} \cdot \frac{A_{s,\text{int}} \cdot f_y}{\lambda \cdot \alpha \cdot f_c \cdot b_w} \right) - \frac{0.318}{FC2 \cdot FC3} \cdot F_r \cdot \left(\frac{DN + h}{2} \right) \tag{19}$$

$$g_1^{SR}(X) = A_{s,\text{int}} \cdot X4 \cdot \left(X2 - X5 - \frac{\phi_{\text{int}}}{2} - \frac{0.8}{2} \frac{A_{s,\text{int}} \cdot X4}{0.68 \cdot X3 \cdot 100} \right) - \frac{0.318}{FC2 \cdot FC3} \cdot F_r \cdot \left(\frac{X1 + X2}{2} \right) \tag{20}$$

The respective LSF for the springline section in pipes with simple reinforcement is:

$$g_2^{SR}(X) = A_{s,\text{int}} \cdot f_y \cdot \left(d'_{l,\text{int}} - \frac{\lambda}{2} \cdot x \right) - \left(\frac{0.182}{FC3} \cdot F_r \cdot r_m - \frac{F_r}{2} \cdot e \right) \tag{21}$$

$$g_2^{SR}(X) = A_{s,\text{int}} \cdot f_y \cdot \left(h - \left(h - c_{\text{int}} - \frac{\phi}{2} \right) - \frac{\lambda}{2} \cdot \frac{A_{s,\text{int}} \cdot f_y}{\lambda \cdot \alpha \cdot f_c \cdot b_w} \right) - \left(\frac{0.182}{FC3} \cdot F_r \cdot \left(\frac{DN + h}{2} \right) - \frac{F_r}{2} \cdot \left(\frac{h}{2} - c_{\text{int}} - \frac{\phi_{\text{int}}}{2} \right) \right) \tag{22}$$

$$g_2^{SR}(X) = A_{s,\text{int}} \cdot X4 \cdot \left(X2 - \left(X2 - X5 - \frac{\phi}{2} \right) - \frac{0.8}{2} \cdot \frac{A_{s,\text{int}} \cdot X4}{0.68 \cdot X3 \cdot 100} \right) - \left(\frac{0.182}{FC3} \cdot F_r \cdot \left(\frac{X1 + X2}{2} \right) - \frac{F}{2} \cdot \left(\frac{X2}{2} - X5 - \frac{\phi_{\text{int}}}{2} \right) \right) \tag{23}$$

The LSF for the crown in RC pipes with double reinforcement (DR) is assumed to be equal to pipes with simple reinforcement since the contribution of the external reinforcement was neglected:

$$g_1^{DR}(X) = A_{s,\text{int}} \cdot X4 \cdot \left(X2 - X5 - \frac{\phi_{\text{int}}}{2} - \frac{0.8}{2} \frac{A_{s,\text{int}} \cdot X4}{0.68 \cdot X3 \cdot 100} \right) - \frac{0.318}{FC2 \cdot FC3} \cdot F_r \cdot \left(\frac{X1 + X2}{2} \right) \tag{24}$$

However, the LSF for the springline section changed due to the axial force being moved to the position of the external reinforcement:

$$g_2^{DR}(X) = A_{s,\text{int}} \cdot f_y \cdot \left(d'_{l,ext} - \frac{\lambda}{2} \cdot x \right) - \left(0.182 \cdot F_r \cdot r_m + \frac{F}{2} \cdot e \right) \tag{25}$$

$$g_2^{DR}(X) = A_{s,ext} \cdot f_y \cdot \left(h - c_{ext} - \frac{\phi_{ext}}{2} - \frac{\lambda}{2} \cdot \frac{A_{s,ext} \cdot f_y}{\lambda \cdot \alpha \cdot f_c \cdot b_w} \right) - \left(0.182 \cdot F_r \cdot \left(\frac{DN + h}{2} \right) + \frac{F}{2} \cdot \left(\frac{h}{2} - c_{ext} - \frac{\phi_{ext}}{2} \right) \right) \tag{26}$$

$$g_2^{DR}(X) = A_{s,ext} \cdot X4 \cdot \left(X2 - X6 - \frac{\phi_{ext}}{2} - \frac{0.8}{2} \cdot \frac{A_{s,ext} \cdot X4}{0.68 \cdot X3 \cdot 100} \right) - \left(\frac{0.182}{FC3} \cdot F_r \cdot \left(\frac{X1 + X2}{2} \right) + \frac{F}{2} \cdot \left(\frac{X2}{2} - X6 - \frac{\phi_{ext}}{2} \right) \right) \tag{27}$$

On which the following nomenclature is applied to the random variables:
X1 = *DN* is nominal diameter of the pipes;
X2 = *h* is pipe thickness;
X3 = f_c, represents the average concrete compressive strength (considering the correction factor FC1 = 1.08);
X4 = f_y, representing the reinforcement yield strength;
X5 = c_{int}, represents the concrete cover of the inner reinforcement layer;
X6 = c_{ext}, represents the concrete cover of the external reinforcement layer (for double-layer reinforcement)

3 Overview of experiments

3.1 RC Pipes used in the three-edge-bearing test (TEBT)

The experimental program used as a reference to estimate the variability of the random variables considered is shown in Silva (2011). This experimental program comprised the test of 32 RC pipes that were divided into 4 groups, detailed in Table 2. In Table 2, DN is the pipe nominal diameter; pipe type refers to spigot and pocket pipes (SPP) and to ogee joint pipe (OJP). *N* refers to the number of pipes tested in each group, $A_{s,int}$ and $A_{s,ext}$ refer to the reinforcement areas of the internal and external layers per unit of pipe length, f_{cm} is the average compressive strength measured in standardized cylinders and *L* is the effective pipe length (without pocket for SPP type).

Table 2 - Characteristics of the tested pipes by Silva (2011) according to ASTM C76 (2016) and NBR 8890:2018 *(ABNT NBR 8890, 2018).*

Serie	Group	DN (mm)	Type	n	h (mm)	$A_{s,int}$ (cm²/m)	$A_{s,ext}$ (cm²/m)	f_{cm} (MPa)	L (m)
1	1	800	SPP	12	72	3.96	-	51.38	1.5
1	2	800	OJP	4	72	3.96	-	51.38	1.2
2	3	1200	SPP	12	110	3.96	1.96	46.80	1.5
2	4	1200	OJP	4	110	3.96	1.96	46.80	1.2

The estimation of the variability of the parameters regarding reinforcement positions (c_{int} and c_{ext}) and wall thicknesses (h) was made by samples retrieved from the pipes at the two ends of the spigot and pocket areas. Cylindric specimens of all tested pipes were extracted by the hole saw (Silva et al., 2018). Since this method may produce microcracking of concrete, which decreases the measured compressive strength, standardized specimens with 100 mm in diameter and 200 mm in height were cast to determine the mechanical properties of concrete. These specimens were subjected to the same curing conditions as the respective pipes. In total, 13 specimens were cast for pipes of 800 mm diameter and 17 specimens with the same concrete used in the pipes of 1200 mm diameter. Table 3 describes the number of measurements, average value and coefficient of variation for the parameter measured.

Table 3 – Parameters measured for Series 1 and 2 of pipes.

Serie 1 - DN 800 mm	h (cm)	c_{int} (cm)	c_{ext} (m)	$f_{c,cast}$ (MPa)	$f_{c,extracted}$ (MPa)	f_y (MPa)
Nº measurements	*32*	*26*	-	*13*	*4*	-
AVG	7.2	2.58	-	51.38	45.5	710
CV (%)	4.2	22.5	-	3.83	20.33	-
Serie 2 - DN 1200 mm	**h (cm)**	**c_{int} (cm)**	**c_{ext} (m)**	**$f_{c,cast}$ (MPa)**	**$f_{c,extracted}$ (MPa)**	**f_y (MPa)**
Nº measurements	32	29	27	16	*32*	-
AVG	10.08	3.35	1.74	46.8	41.3	710
CV (%)	3.90	18.2	31	3.82	13.39	-

3.2 Distribution functions of random variables

In section 2.9, it was assumed the following variables as random ones: X1 = nominal diameter or internal diameter DN; X2 = thickness of the pipe wall h; X3 = compressive strength of concrete f_c; X4 = yielding strength of reinforcement f_y; X5 = concrete cover of the inner or internal reinforcement c_{int} and X6 = concrete cover of the outer reinforcement or external reinforcement c_{ext}.

For the pipes with DN = 800 mm, Silva (2011) verified that the parameters do not follow a normal distribution according to the Shapiro-Wilk normality test (Shapiro & Wilk, 1965). On the other hand, for the pipes with DN = 1200 mm, most parameters were approved in the normality test, including the nominal diameter DN. The only exception was the external concrete cover c_{ext}. This study assumes that all random variables follow normal distributions as a simplification, such as those adopted by Silva et al. (2008) and Silva (2011). Besides that, previous tests assuming log-normal distribution to some parameters such as f_c and c_{int} did not change the results significantly, which motivated the simplification adopted.

The coefficient of variation of the nominal diameter was estimated based on the JCSS (JCSSS Probabilistic Model Code - Part 3: Material Properties, 2001):

$$CV_{DN} = \min\left(\frac{4 + 0.006 \cdot DN}{DN}; \frac{10}{DN}\right) \text{ with DN in mm} \tag{28}$$

The coefficient of variation of the yielding strength of steel was assumed to equal 4%, according to Santiago (2019).

Alternatively, variational Bayesian inference and adaptive Gaussian process modeling could also be used to estimate better the posterior probability distributions of the evaluated structural parameters. To this, the structural response would be used to calibrate the distribution models of parameters. Such examples can be consulted elsewhere (Ni et al., 2021, 2022).

3.3 Monte Carlo simulation

This study adopted a brute force Monte Carlo simulation technique to estimate the failure probability P_f. However, in design code provisions such as the EN 1990:2002 (CEN, 2002), it is more usual to define a required target reliability index β, which is related to the function of the failure probability P_f by inverse normal distribution function:

$$\beta = \Phi^{-1}\left(1 - P_f\right) \tag{29}$$

The number of samples *N* required for a Monte Carlo simulation varies according to the failure probability expected and can be estimated by (Waarts, 2000):

$$N > \frac{3}{p_f} \tag{30}$$

For instance, if the target reliability index β is 4, the required number of samples shall be higher than 10^5, which is commonly the case for the assessment of reinforced concrete structures according to European code provisions (CEN, 2002). In the design of RC structures, the required reliability index of 4 represents a failure probability of 10^{-5}. This failure probability should assume a lower value due to several aspects, such as: (i) to cover well different structures built in different regions from the same country and (ii) balancing the required safety levels by the society with economic aspects.

However, in the manufacturing of RC pipes, the required reliability index β of concrete structures can be replaced by the requirements provided by specific codes related to the acceptance of pipes in standardized tests, such as the one prescribed by the ABNT NBR 8890:2018 (ABNT NBR 8890, 2018), ASTM C947 (ASTM, 2003) and EN 1916:2002 (EN 1916, 2002). Therefore, the required failure probability in a TEBT, for instance, should account for the probability of a chosen pipe between "n" pipes being the one that does not satisfy the TEBT. Consequently, this acceptable failure probability should consider the economic risk assumed by the manufacturer.

In this study, we assume that the failure probability acceptable for the manufacturer could be around 1%. In this way, the required minimum number of samples for MCS is 300 samples. The number of 2000 samples was used in the spreadsheets to improve prediction accuracy.

4 RESULTS

The results focus on the comparison of the longitudinal reinforcement ratios required by three approaches: The traditional approach (TA); Mean Value approach (MVA) and the Rational approach (RA), which are detailed below:

Traditional approach (TA);

- Considers characteristic values (reduced) of the material strength (f_{ck} and f_{yk}) to design the required steel area A_s;
- The partial safety factor γ_f is equal to 1.4;
- For reliability analysis, consider the average values of the material and geometric properties such as (i) nominal diameter of pipes DN, (ii) pipe wall thickness *h* and (iii) reinforcement concrete covers;
- The steel area A_s used in the reliability analyses is equal to the steel area calculated with the characteristic values of the resistances.
- Mean Value approach (MVA):
- Considers average values for the strength of the materials (f_{cm} and f_{ym}) for both design and reliability analysis;
- The value of the average compressive strength of concrete (f_{cm}) is corrected by the factor FC1, to consider the greater compressive strength of the standardized specimens compared to the concrete of pipes after curing.
- Considers partial factor of actions γ_f = 1;
- Rational approach (RA):
- Considers average values (f_{cm} and f_{ym}) for the material properties;
- The value of the average compressive strength of the concrete is still corrected by the factor FC1 to consider the higher compressive strength of the standardized specimens compared to the concrete of the pipes after curing.
- Considers average values for geometric properties;
- The steel reinforcement adopted as a response for the reliability analyses varies according to the rate or probability of failure acceptable by the manufacturer. In other words, firstly, a reinforcement ratio A_s is calculated with the average values of the materials and geometric properties, which corresponds to a failure rate of approximately 50% in the standardized test for the crown section, a procedure similar to the Mean Value Approach (MVA). Subsequently, reinforcement ratios A_s are increased, and the respective failure probabilities are re-calculated. In the end, a graph is reported showing the relation between the reinforcement area and the failure probability.

4.1 Example 1 of results of the proposed method: RC pipes with simple reinforcement

Table 4 shows the input parameters used in the first example. The input parameters from RC with simple reinforcement were chosen mainly based on previous investigations (Silva, 2011; Silva et al., 2018).

Table 5 summarizes the main results from the presented methods: (i) the reinforcement area calculated for each method; (ii) and the respective failure probability for each method using the developed spreadsheet tool. In the Rational Method (RM), an acceptable failure rate of 1% was considered in the calculations.

Table 4 - Input parameters used in Example 1 (pipes with simple reinforcement).

Parameters	RV	AVG	COV	Distribution	Reference for COV
F_r (kN/m)		48	*	-	-
L (m)		1.5	*	-	-
With pocket / without pocket		with	*	-	-
DN (mm)	X1	800	1.10%	normal	(JCSSS - Part 3: Material Properties, 2001)
h (mm)	X2	72	4.20%	normal	(Silva, 2011)
f_{cm} (MPa)	X3	51.4/1.08	3.83%	normal	(Silva, 2011)
f_{ym} (MPa)	X4	600.0	4.00%	normal	(Santiago, 2019; Silva, 2011)
c_{int} (mm)	X5	25.8	22.5%	normal	(Silva, 2011)
ϕ_{int} (mm)		7.1	*	-	-

Notes: AVG = average value; COV = coefficient of variation; RV = random variable; * = determinist value assumed in the example.

As expected, the mean value method presents the lower calculated reinforcement area to resist the TEBT. However, the failure rate is critical (around 50%). In these calculations, the failure rate was slightly larger than 50% because of the two possible failure modes (at the crow or the springline) considered in the joint probability method. On the other hand, the results using the traditional method (TM, with partial safety factors) and the proposed Rational Method (RM) provided close results of $A_{s,int}$ (3.99 cm^2/m with the TM and 3.83cm^2/m with the RM). This occurs mainly because the target failure rate was set as 1% in the rational method, which is close to the one provided by the traditional method. When the failure rate was set to 10%, the $A_{s,int}$ decreased to 2.95 cm^2/m. Therefore, the calculated reinforcement area with p_f = 10% was 36.4% lower than with the traditional method (using partial safety factors).

Figure 10 shows how it works the proposed approach to design the reinforcement area $A_{s,int}$ of RC pipes with simple reinforcement based on the failure probability. The results were plotted as the relation between the reinforcement steel used (the steel increment in relation to the MVM result) and the failure rate. Besides, these graphs show the results of the failure probability at the springline and at the crow sections and combine the results of both in the global failure.

Table 5 - Summary of the results using the Traditional Method (TM, meach value method (MVM) and Rational Method (RM): $A_{s,int}$ *is the calculated steel area and* p_f *is the calculated failure probability for each method.*

Method	Partial factors		Material properties	Coefficients for correction	$A_{s,int}$ (cm^2/m)	p_f (%)
TM	γc	1.4	fck – concrete	FC1 (concrete) = 1	3.99	1.6%
	γs	1.15	fyk – reinforcement	FC2 (load spreading) = 1.085		
	γf	1.4	-	FC3 (pocket) = 1.122		
MVM	γc	1	fcm – concrete	FC1 (concrete) = 1.08	2.22	56.1%
	γs	1	fym – reinforcement	FC2 (load spreading) = 1.085		
	γf	1	-	FC3 (pocket) = 1.122		
RM	γc	1	fcm – concrete	FC1 (concrete) = 1.08	3.83	0.7%
	γs	1	fym – reinforcement	FC2(load spreading) = 1.085		
	γf	1	-	FC3 (pocket) = 1.122		

Figure 10 shows that the failure curve of the springline section is much below the respective failure curve at the crown. This occurs mainly because the bending moment at the crown is the most critical in designing RC pipes with simple reinforcement (see Figure 4). However, Figure 10 also draws attention to the fact that the failure probability in the springline section is considerably high in the MVA result (P_f > 20% for steel increment = 0). This explains why the global failure probability is slightly higher than 50% in MVM, since it accounts for the intersection of failure probabilities. Figure 10 also illustrates that the height of the global failure curve is not the sum of both curves since failures at both the springline and crown are counted only once in the joint failure probability.

It should be highlighted here that the failure probability with the traditional approach (1.6%) is very high compared to the one expected with the safety partial factors method (10^{-5}). These results can be attributed to the higher coefficient of variation of the internal concrete cover (22.5%), which significantly influences members with reduced thickness (h = 72 mm). Note that a coefficient of variation around 22% means a normal standard deviation of approximately 5 mm of the concrete cover, which is well accepted for usual beams and slabs. However, this standard deviation for RC pipes induces a significant variability in the reinforcement position. Comparatively, the JCSS:2001 (Part 3) recommends assuming a standard deviation between 5 and 15 mm for the concrete cover. Therefore, these values should be reviewed for members with reduced thickness.

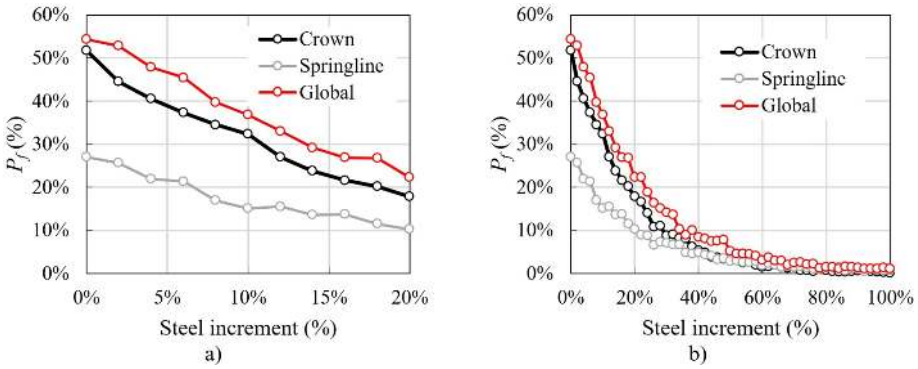

Figure 10 - Failure probability curve for pipe DN 800 SPP according to the increase in steel area in relation to the Mean Value Approach: a) Detail from 0% to 20% of steel increment; b) From 0% to 100% of steel increment.

4.2 Example 2 of results of the proposed method: RC pipes with double-reinforcement

Table 6 shows the input parameters considered for the example of RC pipes with double reinforcement. The mean values and coefficient of variations were inspired mostly by the previous work from Silva et al. (2018) and Santiago (2019).

Table 6 - Input parameters used in Example 2 (pipes with double-reinforcement).

Parameters	RV	AVG	COV	Distribution	Reference for COV
F_r (kN/m)	-	72	*	-	-
L (m)	-	1.5	*	-	-
With pocket / without pocket	-	Without	*	-	-
DN (mm)	X1	1200	0.833%	normal	(JCSSS - Part 3: Material Properties, 2001)
h (mm)	X2	110	3.90%	normal	(Silva, 2011)
f_{cm} (MPa)	X3	46.8/1.08	3.82%	normal	(Silva, 2011)
f_{ym} (MPa)	X4	710	4.00%	normal	(Santiago, 2019; Silva, 2011)
c_{int} (mm)	X5	33.5	22.5%	normal	(Silva, 2011)
c_{ext} (mm)	X6	17.4	31.0%	normal	(Silva, 2011)
ϕ_{int} (mm)	-	7.1	*	-	-
ϕ_{ext} (mm)	-	5.0	*		-

Notes: AVG = average value; COV = coefficient of variation; * = determinist value assumed in the example.

Table 7 summarizes the main results of the proposed analyses, including the reinforcement area calculated for each method and the respective failure probabilities. Figure 11 shows how the failure rate varies as a function of the reinforcement area added in comparison to that calculated in the MVM. In the Rational Method, the target failure rate was set as 1%.

Table 7 - Summary of the results using the Traditional Method (TM), mean value method (MVM) and Rational Method (RM): $A_{s,int}$ *is the calculated steel area and* p_f *is the calculated failure probability for each method.*

Method	Partial factors		Material properties	Coefficients for correction	$A_{s,int}$ (cm^2/m)	$A_{s,ext}$ (cm^2/m)	P_f (%)
TM	γc	1.4	f_{ck} – concrete	FC1 (concrete) = 1.00	4.97	2.74	$<10^{-5}$

	γs	1.15	f_{yk} – reinforcement	FC2 (load spreading) = 1.085			
	γf	1.4	-	FC3 (pocket) = 1			
MVM	γc	1	f_{cm} – concrete	FC1 (concrete) = 1.08	2.77	1.57	52.9%
	γs	1	f_{ym} – reinforcement	FC2 (load spreading) = 1.085			
	γf	1	-	FC3 (pocket) = 1			
RM	γc	1	f_{cm} – concrete	FC1 (concrete) = 1.08	3.93	2.22	0.60%
	γs	1	f_{ym} – reinforcement	FC2 (load spreading) = 1.085			
	γf	1	-	FC3 (pocket) = 1			

Table 7 shows interesting results compared to the pipes with simple reinforcement. Considering all the partial safety factors, the failure rate was much below the target one of 1%. In practice, the failure probability for pipes with double reinforcement using the TM would be similar to that of RC buildings (< 10^{-5}).

The Mean Value Method (MVM) also provided a failure rate of around 50%, as occurred for the pipes with simple reinforcement. On the other hand, the proposed method allowed us to determine the reinforcement area that would satisfy the acceptable failure rate. In this example, the steel area applied should be at least 3.93 cm^2/m in the inner layer and 2.22cm^2/m in the external layer. In other words, the reinforcement area could decrease 20.9% compared to the Traditional Method in the inner layer and 18.9% in the external layer.

Figure 11 shows the respective failure graph for the studied RC pipe. Compared to Figure 10, Figure 11 shows that the failure probability decreases more quickly by increasing the reinforcement area. These results can be attributed mainly to the higher thickness of the members, 110 mm, compared to 72 mm (52% of the increase), which reduces the influence of the variability of the concrete cover in the failure probability.

It is also interesting to note that the difference in height in the failure curves at the springline and at the crown is lower for the RC pipe with double reinforcement (Figure 11) than the simple reinforcement (Figure 10). This occurs because each reinforcement is calculated separately for the pipes with double reinforcement. Consequently, the limit state function at the springline is more critical than the respective one for pipes with simple reinforcement. At this point, it is important to note that for RC pipes with simple reinforcement, the LSF applied at the springline is only a check considering the available reinforcement at the inner layer, which in general, is higher than the required one). On the other hand, for RC pipes with double reinforcement, the LSF at the springline uses only the calculated reinforcement at the external layer. Therefore, the reinforcement area in the external layer for the respective LSF is more limited.

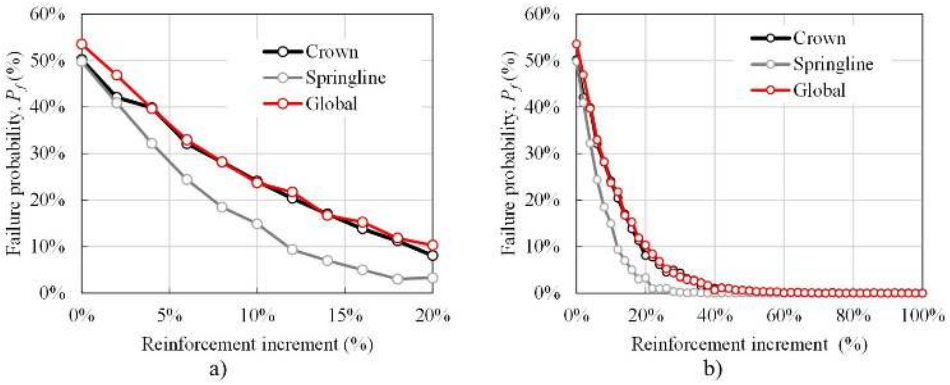

Figure 11 - Failure probability curve for pipe DN 1200 SPP according to the increase in reinforcement area compared to the results of the Mean Value Method (MVM): a) Detail from 0% to 20% of steel increment; b) From 0% to 100% of steel increment.

4.3 Parametric analyses: reliability indices using FORM

Table 8 and Table 9 show how the failure probabilities P_f and reliability indices β vary as a function of the parameter's uncertainties for pipes with simple and double reinforcement, respectively. In Table 8, it was considered the reinforcement area determined in the Traditional Method, while in Table 9 the reinforcement area was determined in the Rational Method with a target failure probability of 10%. This distinction was made because the failure probability in the traditional method for pipes with double reinforcement was already too low. In these analyses, the FORM was applied using the software StrAnd (Beck, 2008).

Table 8 - Influence of the parameters uncertainties on the failure probability and reliability index of LSF1 and LSF2 from pipes with simple reinforcement (Example: DN = 800 mm; h = 72 mm; f_{cm} = 51.4/1.08 MPa; f_{ym} = 600 MPa; c_{int} = 25.8 mm ; A_{sint} = 3.99 cm^2/m)

Parameter		Example 1	Example 2	Example 3	Example 4
		COV (%)	COV (%)	COV (%)	COV (%)
DN	X1	1.1%	1.1%	1.1%	1.1%
h	X2	4.2%	4.2%	4.2%	4.2%
f_{cm}	X3	3.83%	3.83%	3.83%	3.83%
f_{ym}	X4	4.0%	4.0%	4.0%	4.0%
c_{int}	X5	22.5%	15%	10%	5%
Reliability indices		**Example 1**	**Example 2**	**Example 3**	**Example 4**
β_{FORM} (LSF1)		2.57	3.41	4.20	5.04
P_f (LSF1)		$5.11 \cdot 10^{-3}$	$3{,}20 \cdot 10^{-4}$	$1.30 \cdot 10^{-5}$	$2.24 \cdot 10^{-7}$
β_{FORM} (LSF2)		2.45	3.67	5.45	10.07
P_f (LSF2)		$7{,}01 \cdot 10^{-3}$	$1{,}20 \cdot 10^{-4}$	$2.52 \cdot 10^{-8}$	$< 10^{-10}$

Table 8 shows that by decreasing the coefficient of variation of the concrete cover and, hence, the uncertainty on the reinforcement position, the reliability index increases considerably. In this example, the reliability of LSF1 increased from 2.57 to 5.04 when the coefficient of variation of c_{int} was decreased from 22.5% to 5%. Therefore, enhanced levels of safety for pipes with simple reinforcement can be achieved by improving the methods related to reinforcement installation in the pipes.

Similarly, Table 9 also highlights that enhanced levels of safety (higher values of reliability index) can be achieved decreasing the coefficients of variation related to the concrete cover. The reader may also note that, by decreasing the coefficients of variation related to the reinforcement position, it is possible to achieve in Example 3 the same level of failure probability (P_f = 7.23 ·10-3 ≈ 1%) from the rational method for a target 1% failure rate but without increasing the reinforcement area.

Table 9 - Influence of the parameters uncertainties on the failure probability and reliability index β of LSF1 and LSF2 from pipes with double reinforcement (Example: DN = 1200 mm; h = 110 mm; f_{cm} = 46.8/1.08 MPa; f_{ym} = 710 MPa; c_{int} = 33.5 mm; $A_{s,int}$ = 3.38 cm^2/m; $A_{s,ext}$ = 1.91 cm^2/m – Rational Method with p_f target as 10%)

Parameter		Example 1	Example 2	Example 3
		COV (%)	COV (%)	COV (%)
DN	X1	0.833%	0.833%	0.833%
h	X2	3.9%	3.9%	3.9%
f_{cm}	X3	3.82%	3.82%	3.82%
f_{ym}	X4	4.0%	4.0%	4.0%
c_{int}	X5	18.0%	9.0%	4.5%
c_{ext}	X6	31.0%	15%	7.5%
Reliability indices		**Example 1**	**Example 2**	**Example 3**
β_{FORM} (LSF1)		1.58	2.16	2.44
P_f (LSF1)		$5.65 \cdot 10^{-2}$	$1.51 \cdot 10^{-2}$	$7.23 \cdot 10^{-3}$
β_{FORM} (LSF2)		2.59	3.12	3.28
P_f (LSF2)		$4.71 \cdot 10^{-3}$	$8.90 \cdot 10^{-4}$	$5.02 \cdot 10^{-4}$

4.4 Sensitivity analyses using FORM

In this section, the First Order Reliability Method (FORM) was applied with the Strand Software (Beck, 2008) to calculate the sensitivity factors (SF) of the random variables. The value of the sensitivity factor indicates the relative contribution of the random variable to the failure probability (Bairán et al., 2021) of each limit state function (LSF). In this study, LSF1 refers to the crown section and LSF2 refers to the springline section. The reinforcement ratios used in the limit state functions refer to the values calculated in the TM for pipes with simple reinforcement and RM for pipes with double reinforcement (same assumptions from Section 4.3).

Table 10 and Table 11 show a summary of results obtained for the sensitivity factor of the parameters studied in the probability of failure of pipes with simple reinforcement and double reinforcement, respectively. In these analyses, StrAnD Software was used (Beck, 2008).

Table 10 shows that the sensitivity factor of the parameters depends strongly on the coefficient of variation (COV) or variability of them in relation to the set. In the Reference set, using the coefficients of variation based on experimental measurements from previous studies, someone can realize that the concrete internal cover c_{int} has the largest influence on the failure probability (78% for LSF1 and 99% for LSF2). The second parameter with the largest relative contribution to the failure probability is the tube thickness *h*, which in the Reference set was around 20% for LSF1. Table 10 also shows that decreasing the coefficient of variation of c_{int} from 22.5% to 5% decreases the sensitivity factor from around 78% to around 14% in LSF1. On the other hand, the decrease of the SF in LSF2 is less accentuated. In this case, the SF was 70% for LSF2. Besides, Table 10 also shows that decreasing the coefficient of variation of c_{int} increases the relative contribution of the pipe thickness *h* almost in the same proportion for LSF1. Therefore, in order to achieve better reliability of RC pipes at the TEBT, it is fundamental to decrease the uncertainties of c_{int}.

Table 10 – Sensitivity factor (SF) of the parameters on the failure probability of pipes with simple reinforcement (Example: DN = 800 mm; h = 72 mm; f_{cm} = 51.4/1.08 MPa; f_{ym} = 600 MPa; c_{int} = 25.8 mm ; A_{sint} = 3.99 cm^2/m).

Parameter	RV	Reference			Example 1			Example 2			Example 3		
		COV (%)	SF (%) - LSF1	SF (%) - LSF2	COV (%)	SF (%) - LSF1	SF (%) - LSF2	COV (%)	SF (%) - LSF1	SF (%) - LSF2	COV (%)	SF (%) - LSF1	SF (%) - LSF2
DN	X1	1.1	0.12	0.08	1.1	0.22	0.17	1.1	0.35	0.40	1.1	0.53	1.81
h	X2	4.2	20.10	0.03	4.2	35.49	0.09	4.2	53.71	0.20	4.2	77.39	0.92
f_{cm}	X3	3.83	0.03	0.05	3.83	0.05	0.10	3.83	0.07	0.22	3.83	0.11	0.50
f_{ym}	X4	4.0	1.54	0.51	4.0	2.84	1.19	4.0	4.54	2.99	4.0	7.08	26.05
c_{int}	X5	22.5	78.19	99.33	15	61.38	98.44	10	41.3	96.18	5	14.89	70.71

Note: RV = Random Variable; SF = sensitivity factor; LSF1 = Limit State Function 1 (crown section); LSF2 = Limit State Function 2 (springline section).

Table 11 shows how the sensitivity factors vary as a function of the coefficient of variation of the internal and external concrete cover (c_{int} and c_{ext}). Note that, as the external reinforcement is neglected in the calculation of the internal reinforcement, and vice-versa, the relative contribution of c_{ext} to the failure probability of LSF1 is 0. In the same way, the SF of c_{int} to the failure probability of LSF2 is also 0.

Table 11 shows that, as occurs for the pipes with simple support, the relative contribution of c_{int} to the failure probability at the crow section (LSF1) decreases significantly as the coefficient of variation decreases. In the same way, the relative contribution or the sensitivity factor of the pipe thickness increases as the coefficient of variation c_{int} decreases.

Table 11 – Sensitivity factor (SF) of the parameters on the failure probability of LSF1 from pipes with double reinforcement (Example: DN = 1200 mm; h = 110 mm; f_{cm} = 46.8/1.08 MPa; f_{ym} = 710 MPa; c_{int} = 33.5 mm; $A_{s,int}$ = 3.38 cm^2/m; $A_{s,ext}$ = 1.91 cm^2/m – Rational Method with p_f target as 10%).

Parameter	RV	Reference			Example 1			Example 2		
		COV (%)	SF (%) - LSF1	SF (%) - LSF2	COV (%)	SF (%) - LSF1	SF (%) - LSF2	COV (%)	SF (%) - LSF1	SF (%) - LSF2
DN	X1	0.833	0.34	0.71	0.833	0.65	1.05	0.83	0.85	1.17
h	X2	3.9	28.72	33.08	3.9	53.13	45.43	3.9	67.05	48.97
f_{cm}	X3	3.82	0.025	0.012	3.82	0.045	0.016	3.82	0.056	0.017
f_{ym}	X4	4.0	8.71	24.76	4.0	17.35	40.30	4.0	22.93	46.29
c_{int}	X5	18.0	62.19	0	9.0	28.81	0	4.5	9.10	0
c_{ext}	X6	31.0	0	41.42	15.5	0	13.19	7.5	0	3.54

Note: RV = Random Variable; SF = sensitivity factor; LSF1 = Limit State Function 1 (crown section); LSF2 = Limit State Function 2 (springline section).

5 CONCLUSIONS

In this study, we discuss the design of RC pipes under TEBT based on probabilistic analyses. Compared to previous publications, we discuss more clearly some aspects, such as the significance of the external reinforcement in pipes with

double reinforcement and the effect of variability of the concrete cover in pipes with simple reinforcement. The following conclusions can be drawn:

- The reliability-based design proposed is a helpful tool for manufacturers of reinforced concrete pipes since it provides a rational approach for decision-making on required reinforcement in pipes based on the balance of risk and safety judged by the manufacturer.
- In general, a higher failure rate p_f is observed in the design of RC pipes with simple reinforcement compared to that expected for RC buildings members using the partial safety factors. In this study, this occurs mainly due to the large coefficient of variation of the reinforcement position (related to the concrete cover c_{int}), which for members with reduced thickness, which increases the failure rate of the members. Using the FORM and coefficient of variation measured on experimental studies, the sensitivity factors of the concrete cover c_{int} to the failure probability at the crown section were around 75% and 65% for pipes with simple and double reinforcement, respectively.
- In the design of pipes with simple reinforcement, using the traditional methods (with partial safety factors from buildings) provided a failure probability of around 1.6% at the TEBT. Depending on the acceptable level of failure (judged by the manufacturer), the needed reinforcement ratio can increase or decrease. For instance, accepting a failure rate at the TEBT of 10%, the calculated reinforcement area may decrease by more than 30% for pipes with simple reinforcement.
- In the design of RC pipes with double-layer reinforcement, the traditional design method resulted in a failure probability lower than 10^{-5}, considerably lower compared to the respective rate for pipes with simple reinforcement. This occurs because the larger pipe thickness decreases the influence of the concrete cover uncertainties in the reinforcement position and also because the reinforcement area needed at the crown and springline sections is calculated separately, which increases safety from the overall process.
- The failure rate decreases more quickly for pipes with double reinforcement as the reinforcement steel increases compared to the pipes with simple reinforcement.
- In pipes with simple reinforcement and using average values of material properties, the failure rate of the crown section is around 50% (as expected), and the failure rate at the springline section is around 20%. Therefore, the crown section is also more critical based on probabilistic analyses. However, considering both Limit State Functions did not considerably increase the failure rate for the pipes in the presented method. This occurs because, usually, when the springline fails, the crown section also fails. Similar behavior occurs for the pipes with double reinforcement.
- In the industry, the best way to improve the reliability of the pipes to satisfy the TEBT is to reduce the uncertainties related to the concrete cover of the rebars. Making this, a more economical design of the pipes can be achieved using probabilistic methods.

Acknowledgments

The authors gratefully acknowledge the financial support provided by the National Council for Scientific and Technological Development (CNPq), the São Paulo Research Foundation (FAPESP #2021/13916-0) and the Associação Brasileira dos Fabricantes de Tubos de Concreto (ABTC). This study was also financed in part by the Coordenação de Aperfeiçoamento de Pessoal de Nível Superior – Brasil (CAPES) – Finance Code 001. The authors also gratefully acknowledge professor André Beck for providing the software StrAnd used in the analyses.

Author's Contribuitions: Conceptualization, AMD de Sousa and MK El Debs; Methodology, AMD de Sousa, LP Prado and MK El Debs; Investigation, AMD de Sousa, LP Prado and MK El Debs; Writing - original draft, AMD de Sousa, LP Prado and MK El Debs; Writing - review & editing, AMD de Sousa, LP Prado and MK El Debs; Funding acquisition, AMD de Sousa and MK El Debs; Resources, AMD de Sousa and MK El Debs; Supervision, AMD de Sousa and MK El Debs.

Editor: Pablo Andrés Muñoz Rojas

References

AASHTO. (2017). AASHTO LRFD Bridge Design Specifications (8th Editio). American Association of State Highway and Transportation Officials (AASHTO).

ABNT NBR 6118. (2014). NBR 6118: Design of concrete structures — Procedure (in portuguese). Asso-ciação Brasileira de Normas Técnicas (ABNT).

ABNT NBR 8681. (2003). Ações e segurança nas estruturas - Procedimento. Associação Brasileira de Normas Técnicas, 22. https://doi.org/01.080.10; 13.220.99

ABNT NBR 8890. (2018). Concrete pipe for drainage and sewer systems — Requirements and test methods (in Portuguese). In Associação Brasileira de Normas Técnicas. Associação Brasileira de Normas Técnicas. https://doi.org/01.080.10; 13.220.99

ABNT NBR 9062. (2017). Projeto e execução de estruturas de concreto pré-moldado. Associação Brasi-leira de Normas Técnicas, 86. https://doi.org/01.080.10; 13.220.99

Abolmaali, A., Mikhaylova, A., Wilson, A., & Lundy, J. (2012). Performance of steel fiber-reinforced concrete pipes. Transportation Research Record, 2313, 168–177. https://doi.org/10.3141/2313-18

ASTM. (2003). ASTM-C497-03a: Standard Test Methods for Concrete Pipe, Manhole Sections, or Tile. American Society for Testing and Materials (ASTM).

ASTM. (2016). ASTM-C76-16: Standard Specification for Reinforced Concrete Culvert, Storm Drain, and Sewer Pipe. American Society for Testing and Materials (ASTM).

ASTM C497-13. (2013). Standard Test Methods for Concrete Pipe, Manhole Sections or Tile. ASTM In-ternational, West Conshohocken, PA.

Bairán, J. M., Tošić, N., & de la Fuente, A. (2021). Reliability-based assessment of the partial factor for shear design of fibre reinforced concrete members without shear reinforcement. Materials and Struc-tures 2021 54:5, 54(5), 1–16. https://doi.org/10.1617/S11527-021-01773-Z

Beck, A. T. (2008). StRAnD, Structural Reliability Analysis and Design. Engenharia de Estruturas. Escola de Engenharia de São Carlos, USP.

CEN. (2002). Eurocode – Basis of structural design, EN 1990:2002 (p. 119). Comité Européen de Norma-lisation.

Das, B. M., & Seeley, G. R. (1975). Breakout resistance of shallow horizontal anchors J. Geotech. Eng., ASCE, 101 (9) (1975), pp. 999-1003. Journal of Geotechnical Engineering, ASCE, 101(9), 999–1003.

El Debs, M. K. (2003). Projeto Estrutural de Tubos Circulares de Concreto Armado.

EN 1916. (2002). Concrete pipes and fittings, unreinforced, steel fibre and reinforced. Comité Européen de Normalisation.

Figueiredo, A. D. de, Fuente, A. de la, Aguado, A., Molins, C., & Chama Neto, P. J. (2012). Steel fiber reinforced concrete pipes: part 1: technological analysis of the mechanical behavior. Revista IBRA-CON de Estruturas e Materiais, 5(1), 1–11. https://doi.org/10.1590/s1983-41952012000100002

Fusco, P. B. (2008). Tecnologia do Concreto Estrutural : Tópicos Aplicados (1o Edição). Editora PINI LTDA.

Fusco, P. B. (2012). Controle da resistência do concreto. ABECE Informa, 89, p.12-19.

JCSSS Probabilistic Model Code - Part 3: Material Properties, 73 (2001). https://doi.org/10.1093/jicru/ndm007

Kataoka, M. N., da Silva, J. L., de Oliveira, L. M. F., & el Debs, M. K. (2017). FE analysis of RC pipes under three-edge-bearing test: Pocket and diameter influence. Computers and Concrete, 20(4), 483–490. https://doi.org/10.12989/cac.2017.20.4.483

Ladanyi, B., & Hoyaux, B. (1969). A study of the trap-door problem in a granular mass. Canadian Ge-otechnical Journal, 6(1), 1–14. https://doi.org/10.1139/t69-001

Li, Y. G. (2009). Study on Unified Calculation Theory of Earth Pressure on Top of Trench-Buried Culverts and Positive-Buried Culverts. Taiyuan University of Technology (Ph.D. thesis), Taiyuan.

MacDougall, K., Hoult, N. A., & Moore, I. D. (2016). Measured load capacity of buried reinforced con-crete pipes. ACI Structural Journal, 113(1), 63–74. https://doi.org/10.14359/51688059

Marston, A., & Anderson, A. O. (1913). The Theory of Loads on Pipes in Ditches and Tests of Cement and Clay Drain Tile and Sewer Pipe. Iowa State College of Agriculture and Mechanic Arts.

Matyas, E. L., & Davis, J. B. (1983). Experimental Study of Earth Loads on Rigid Pipes. Journal of Ge-otechnical Engineering, 109(2), 202–209. https://doi.org/10.1061/(ASCE)0733-9410(1983)109:2(202)

Melchers, R. E., & Beck, A. T. (2018). Structural reliability: analysis and prediction (3rd Ed). John Wiley & Sons.

Meyerhof, G. G., & Adams, J. I. (1968). The Ultimate Uplift Capacity of Foundations. Canadian Ge-otechnical Journal, 5(4), 225–244. https://doi.org/10.1139/t68-024

Mohamed, N., Soliman, A. M., & Nehdi, M. L. (2015). Mechanical performance of full-scale precast steel fibre-reinforced concrete pipes. Engineering Structures, 84, 287–299. https://doi.org/10.1016/j.engstruct.2014.11.033

Monte, R., de La Fuente, A., de Figueiredo, A. D., & Aguado, A. (2016). Barcelona test as an alternative method to control and design fiber-reinforced concrete pipes. ACI Structural Journal, 113(6), 1175–1184. https://doi.org/10.14359/51689018

Ni, P., Han, Q., Du, X., & Cheng, X. (2022). Bayesian model updating of civil structures with likelihood-free inference approach and response reconstruction technique. Mechanical Systems and Signal Pro-cessing, 164. https://doi.org/10.1016/j.ymssp.2021.108204

Ni, P., Li, J., Hao, H., Han, Q., & Du, X. (2021). Probabilistic model updating via variational Bayesian inference and adaptive Gaussian process modeling. Computer Methods in Applied Mechanics and Engineering, 383. https://doi.org/10.1016/j.cma.2021.113915

Park, Y., Abolmaali, A., Mohammadagha, M., & Lee, S. (2015). Structural performance of dry-cast rub-berized concrete pipes with steel and synthetic fibers. Construction and Building Materials, 77, 218–226. https://doi.org/10.1016/j.conbuildmat.2014.12.061

Peyvandi, A., Soroushian, P., & Jahangirnejad, S. (2013). Enhancement of the structural efficiency and performance of concrete pipes through fiber reinforcement. Construction and Building Materials, 45, 36–44. https://doi.org/10.1016/j.conbuildmat.2013.03.084

Peyvandi, A., Soroushian, P., & Jahangirnejad, S. (2014). Structural design methodologies for concrete pipes with steel and synthetic fiber reinforcement. ACI Structural Journal, 111(1), 83–91. https://doi.org/10.14359/51686432

Ramadan, A., Younis, A. A., Wong, L. S., & Nehdi, M. L. (2020). Investigation of structural behavior of precast concrete pipe with single elliptical steel cage reinforcement. Engineering Structures, 219(April), 110881. https://doi.org/10.1016/j.engstruct.2020.110881

Rikabi, F. T., Sargand, S. M., Kurdziel, J., & Hussein, H. H. (2018). Experimental investigation of thin-wall synthetic fiber-reinforced concrete pipes. ACI Structural Journal, 115(6), 1671–1681. https://doi.org/10.14359/51702413

Santiago, W. C. (2019). Calibração Baseada Em Confiabilidade Dos Coeficientes Parciais De Segurança Das Principais Normas Brasileiras De Projeto Estrutural. Universidade de São Paulo - Escola de Engenharia de São Carlos.

Shapiro, S. S., & Wilk, M. B. (1965). An Analysis of Variance Test for Normality (Complete Samples). Biometrika, 52(3/4), 611. https://doi.org/10.2307/2333709

Shmulevich, I., Galili, N., & Foux, A. (1986). Soil Stress Distribution around Buried Pipes. Journal of Transportation Engineering, 112(5), 481–494. https://doi.org/10.1061/(ASCE)0733-947X(1986)112:5(481)

Silva, J. L. da. (2011). Análise de tubos circulares de concreto armado para o ensaio de compressão dia-metral com base na teoria de confiabilidade [Thesis]. University of São Paulo.

Silva, J. L., Debs, M. K. E. L., & Beck, A. T. (2008). Reliability Evaluation of Reinforced Concrete Pipes in Crack Opening Limit State. IBRACON Structures and Materials Journal, 1(4), 314–321.

Silva, J. L., el Debs, M. K., & Kataoka, M. N. (2018). Investigação experimental de tubos de concreto armado submetidos ao ensaio de compressão diametral: Tipo ponta e bolsa e macho-fêmea. Acta Sci-entiarum - Technology, 40, 1–7. https://doi.org/10.4025/actascitechnol.v40i1.30860

Spangler, M. G. (1941). The Structural Design of Flexible Pipe Culverts. Iowa State College of Agricul-ture and Mechanic Arts.

Tian, W.-D. (1989). The review of vertical earth pressure theory on the buried culvert in recent years at home and abroad. Zhe Jiang Hydrotech., 1(13–21). https://www.scopus.com/record/display.uri?eid=2-s2.0-77955339017&origin=inward&txGid=dfbf2e0464eb08674c85af50e91190ac

Tian, Y., Liu, H., Jiang, X., & Yu, R. (2015). Analysis of stress and deformation of a positive buried pipe using the improved Spangler model. Soils and Foundations, 55(3), 485–492. https://doi.org/10.1016/j.sandf.2015.04.001

Vesic, A. S. (1971). Breakout resistance of objects embedded in ocean bottom. Journal of the Soil Me-chanics and Foundations Division, ASCE, 97(9), 1183–1205.

Waarts, P. H. (2000). Structural reliability using Finite Element Analysis - An appraisel of DARS: Direc-tional Adaptive Response surface Sampling. Delft University Press.

Wilson, A., & Abolmaali, A. (2014). Performance of synthetic fiber-reinforced concrete pipes. Journal of Pipeline Systems Engineering and Practice, 5(3). https://doi.org/10.1061/(ASCE)PS.1949-1204.0000166